

# One-dimensional thermal model for direct methanol fuel cell stacks Part II. Model based parametric analysis and predicted temperature profiles

P. Argyropoulos, K. Scott<sup>\*</sup>, W.M. Taama

*Chemical and Process Engineering Department, University of Newcastle upon Tyne, Merz Court, Newcastle upon Tyne, NE1 7RU, UK*

Received 24 August 1998; accepted 27 December 1998

## Abstract

Using the one-dimensional thermal model for the direct methanol fuel cell (DMFC) (presented in Part I), based on the differential thermal energy conservation equation, which describes the thermal behaviour of a DMFC stack comprised of up to 25 large (272 cm<sup>2</sup>) cells, temperature profiles are predicted along the stack length. The model is used to assess the effect of operating parameters (temperature gradient, current density, flow rate and pressure) on the temperature profile along the stack. In addition, it enables investigation of the stack thermal management and the effect of altering a number of systematic parameters such as the number of cells in the stack, the active and exposed area and the interactions between the physical properties of the various components. The model aids the fuel cell system designer to gain an insight in the stack structure and select materials and geometric configurations that are optimal from a thermal management point of view. © 1999 Elsevier Science S.A. All rights reserved.

*Keywords:* Direct methanol fuel cell; Polymer electrolyte membrane; Thermal modelling; Temperature profile

## 1. Introduction

Fuel cells that can operate directly on fuels such as methanol are attractive for low to medium power applications in view of their low weight and volume relative to other power sources. The weight and volume advantages of direct oxidation fuel cells are due to the fact that they do not require any fuel processing equipment. Elimination of the fuel processor results in simpler design and operation, higher reliability, less maintenance and lower capital and operating costs. Further direct oxidation fuel cells are projected to have rapid and multiple start-up capabilities, and the ability to easily follow varying loads.

A liquid feed direct methanol fuel cell (DMFC) has been developed based on proton-exchange membrane electrolyte and Pt/Ru and Pt catalysed fuel cell and Air/O<sub>2</sub> electrodes, respectively [1]. The cell has been shown to deliver significant power outputs (> 100 mW cm<sup>-2</sup>) at temperatures of 60–90°C.

In order for these fuel cell systems to become efficient and affordable sources of electrical power a greater under-

standing of complete fuel cell systems, and the many parameters that affect them is needed. Experimental investigation of each one parameter would be costly and time consuming and thus a model based study has been undertaken to overcome these limitations. Such a mathematical model was developed in Part I, for a liquid feed DMFC stack, based on the differential thermal energy conservation equation. The model describes the thermal behaviour of the cell stack using material and energy balances posed initially in one dimension, along the length of the stack. This enables estimations of the temperature profile and the interactions between the various components in the cell stack.

The thermal model is used, in this paper, to assess the effect of the fuel condition (liquid or vapour), operating conditions, cell component physical properties and geometrical dimensions on the stack thermal management and performance.

## 2. Parametric analysis methodology

Recently, we have presented experimental results for optimisation of the DMFC based on the effect of operation conditions on a small scale (9 cm<sup>2</sup>) cells performance

<sup>\*</sup> Corresponding author

[1,2]. From the conclusions of these studies, a number of operating parameters are selected to assess their effect on cell thermal behaviour. A base case scenario was selected for a fuel cell stack of three cells (625 cm<sup>2</sup> total cross-section). For the anode side, these conditions are: 1.0 dm<sup>3</sup> min<sup>-1</sup> methanol aqueous solution volumetric flow rate per cell, 2.0 M methanol concentration, 80°C solution inlet temperature, and a current density of 100 mA/cm<sup>2</sup>. In the case of the cathode side, these are 2 barg cathode pressure, 22°C air inlet temperature, and 1.0 dm<sup>3</sup> min<sup>-1</sup> air volumetric flow rate per cell. The range of parameter investigation was dictated from the operating range already pro-

posed for our stack and the economics of the overall process.

### 3. System based parameters

There are several parameters that can be changed in the system: material physical properties (i.e., electrical resistivity, thermal conductivity), geometrical details (layer thickness, active area, flow bed design), the number of cells in the stack body, operating current density and the end block configuration. The term end block defines the part of the

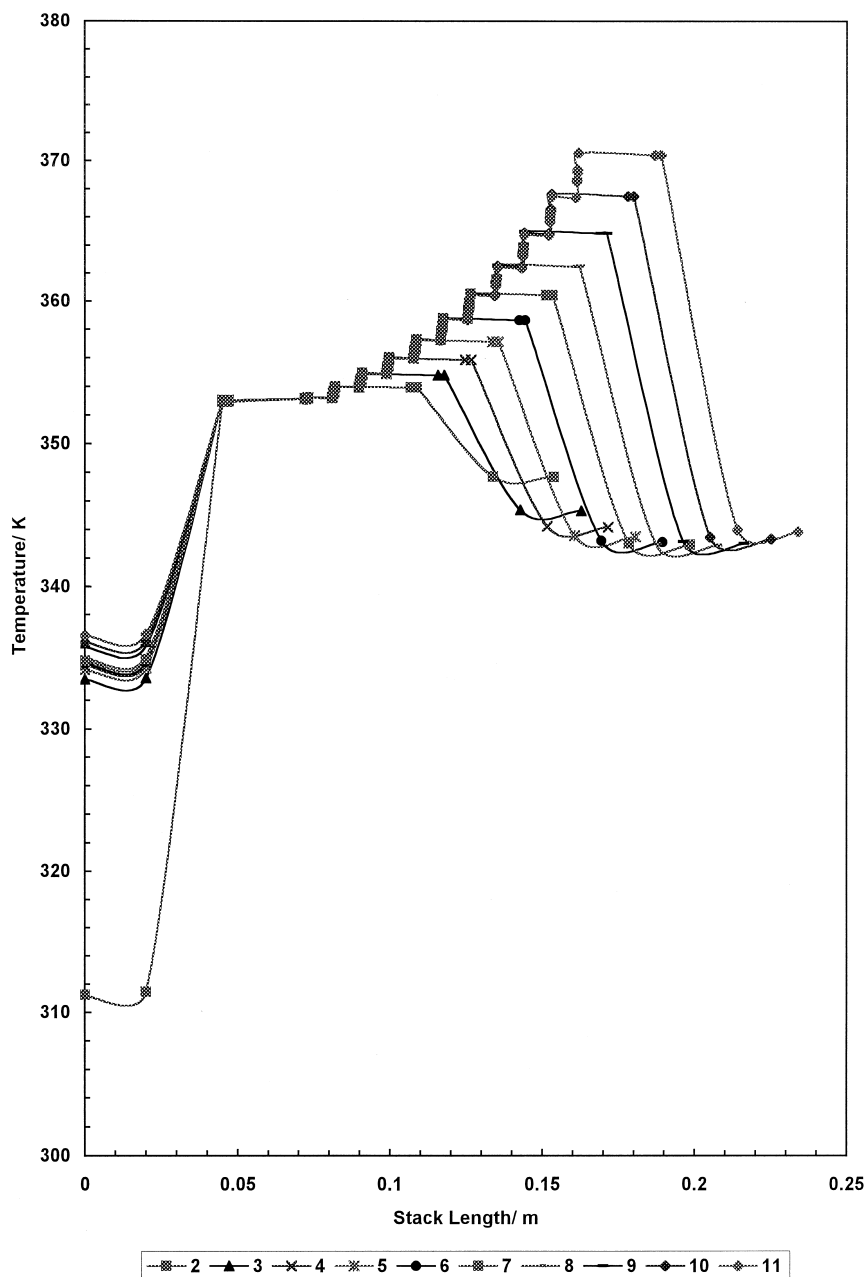


Fig. 1. Longitudinal temperature profiles for increasing number of stacked cells (1–11) at 80°C anode side inlet temperature, 20° cathode side inlet temperature, current density 100 mA cm<sup>-2</sup>, anode and cathode inlet flow rate 1.0 dm<sup>3</sup> min<sup>-1</sup> per cell, 2 bar cathodic pressure.

stack structure, which exist before the first cell anode side gas diffusion layer and after the last cell cathode side diffusion layer.

Despite the fact that altering one of the aforementioned parameters can affect the cell performance it is expected that the number of cells in the stack, the operating current density and the ratio of the active area (i.e., the area covered with an electrocatalyst layer) to the block cross-section area, are the most important ones. For instance, changing the electrical resistivity of any layer will greatly affect the electrical performance of the cell but it will not change dramatically the heat produced from that layer due

to its ohmic resistance. As will be shown below that kind of heat source do not play an important role in the stack thermal management.

Fig. 1 presents stack temperature profiles as a function of increasing stack length for a range of cells present in the stack. The configuration of the stack is such that from the left-hand side the first electrode is the anode. As it can be seen increasing the number of cells results in a gradual increase in the average stack temperature (around  $10^{\circ}\text{C}$  for every 10 cells). Heat losses from the end block are almost constant and independent of the number of cells present in the stack except in the case of a two-cell stack. In this

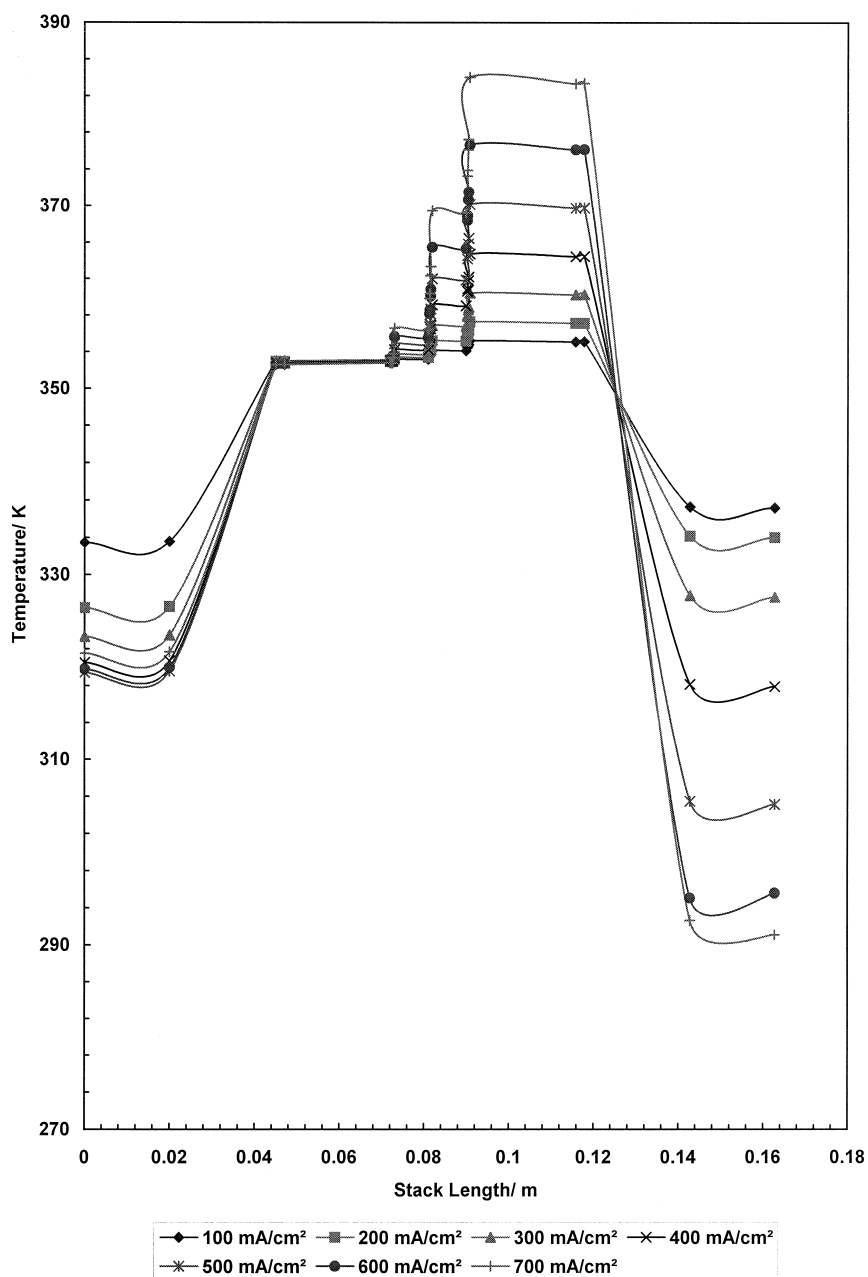


Fig. 2. Three-cell stack longitudinal temperature profiles for increasing operating current density at  $80^{\circ}\text{C}$  anode side inlet temperature,  $20^{\circ}$  cathode side inlet temperature, anode and cathode inlet flow rate  $1.0 \text{ dm}^3 \text{ min}^{-1}$  per cell, 2 bar cathodic pressure.

case, there is a different behaviour attributed to the large heat losses from the two end blocks in comparison with the overall heat balance. Heat is flowing continuously from the cell anode side to the cathode side mainly through the electroosmotic flow of water and methanol in the same direction. Heat that cannot be removed from the cathode side air-flow is transferred through the bipolar plate to the next cell and hence the gradually increasing temperature profile. It is frequently reported in the literature that there is a problem with the temperature of either the first or the last cell in the stack, attributed to the effect of heat loss

from the end blocks [3]. Since we are using a relatively high flow rate of preheated methanol solution, it is expected (and it is verified from the graph) that the losses from the end blocks will be easily replenished from the large amount of heat provided from the inlet stream. It should be pointed out that with low flow rates this problem is more intense and could result in serious electrical performance deterioration. The stack main body lower temperature is mainly determined from the inlet temperature of the fuel. Hence, by controlling the inlet temperature of the feed we can achieve some control of the stack's overall

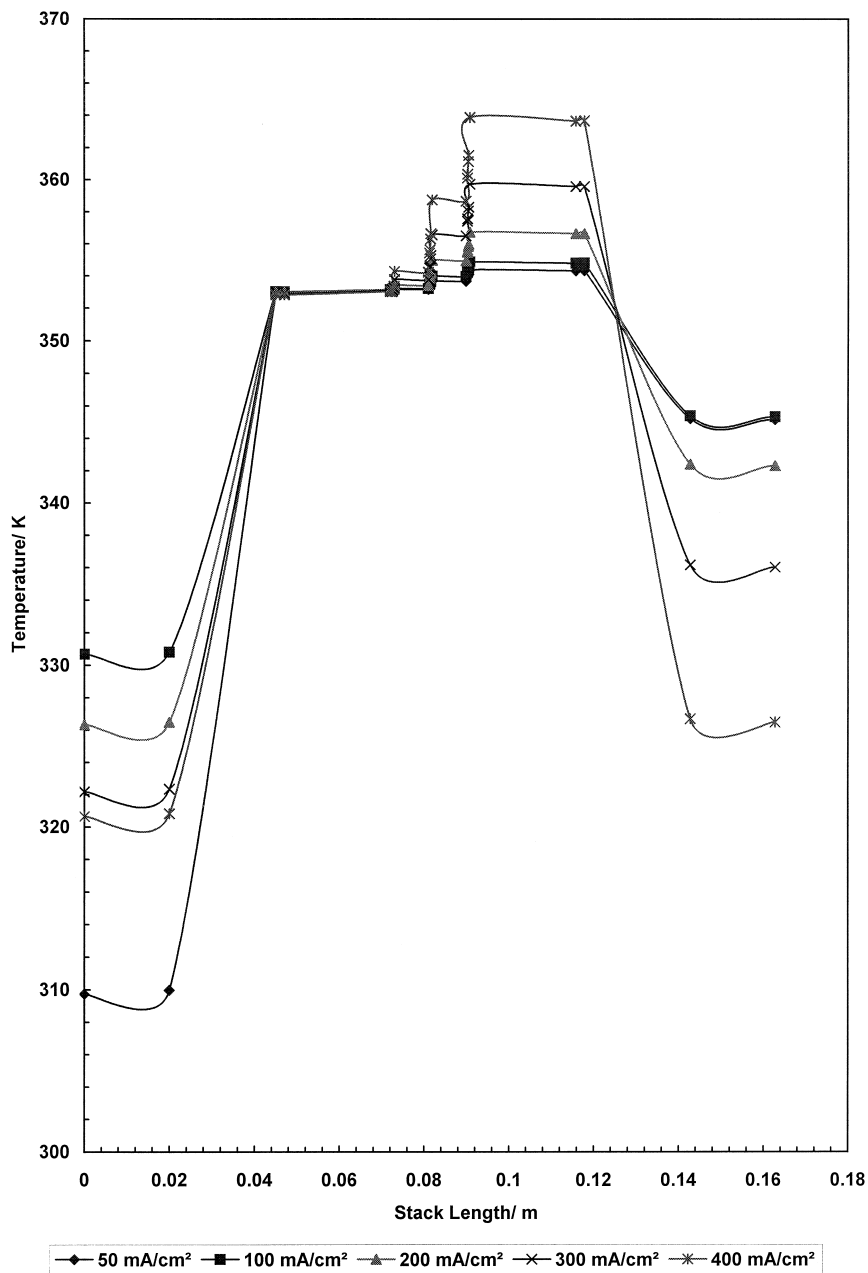


Fig. 3. Three-cell stack longitudinal temperature profiles for increasing operating current density at 80°C anode side inlet temperature, 20°C cathode side inlet temperature, current density 100 mA cm<sup>-2</sup>, anode inlet flow rate 1.0 dm<sup>3</sup> min<sup>-1</sup> per cell, cathode inlet flow rate 2.0 dm<sup>3</sup> min<sup>-1</sup> per cell, 2 bar cathode air pressure.

thermal management. Increasing the number of the cells present in the stack creates an increasing demand for heat removal from the stack main body. These problem can be managed by increasing the feed inlet flow rate, decreasing the inlet temperature, or with the use of inter-cell cooling plates. An implication of the temperature variation in stacks with a large number of cells is the variation in electrochemical performance in each cell that will occur. The electrochemical performance furthermore dictates the amount of heat liberated at the two half-cells. Although the present model treats all cells as being at a steady state,

with a constant and identical electrochemical performance, large temperature variations inside the stack will lead to a non-uniform operating system. Furthermore, when the temperature exceeds approximately  $100^{\circ}\text{C}$ , a change in the system occurs, depending upon pressure, from a liquid-fed system to a vapour fed cell, with properties and characteristics that are a lot different than those of the liquid system. An additional factor, which we are exploring in current work, is the flow distribution, which will occur in fuel cell stacks through the manifold arrangement of the cells. The manifolding of many cells will cause a variation

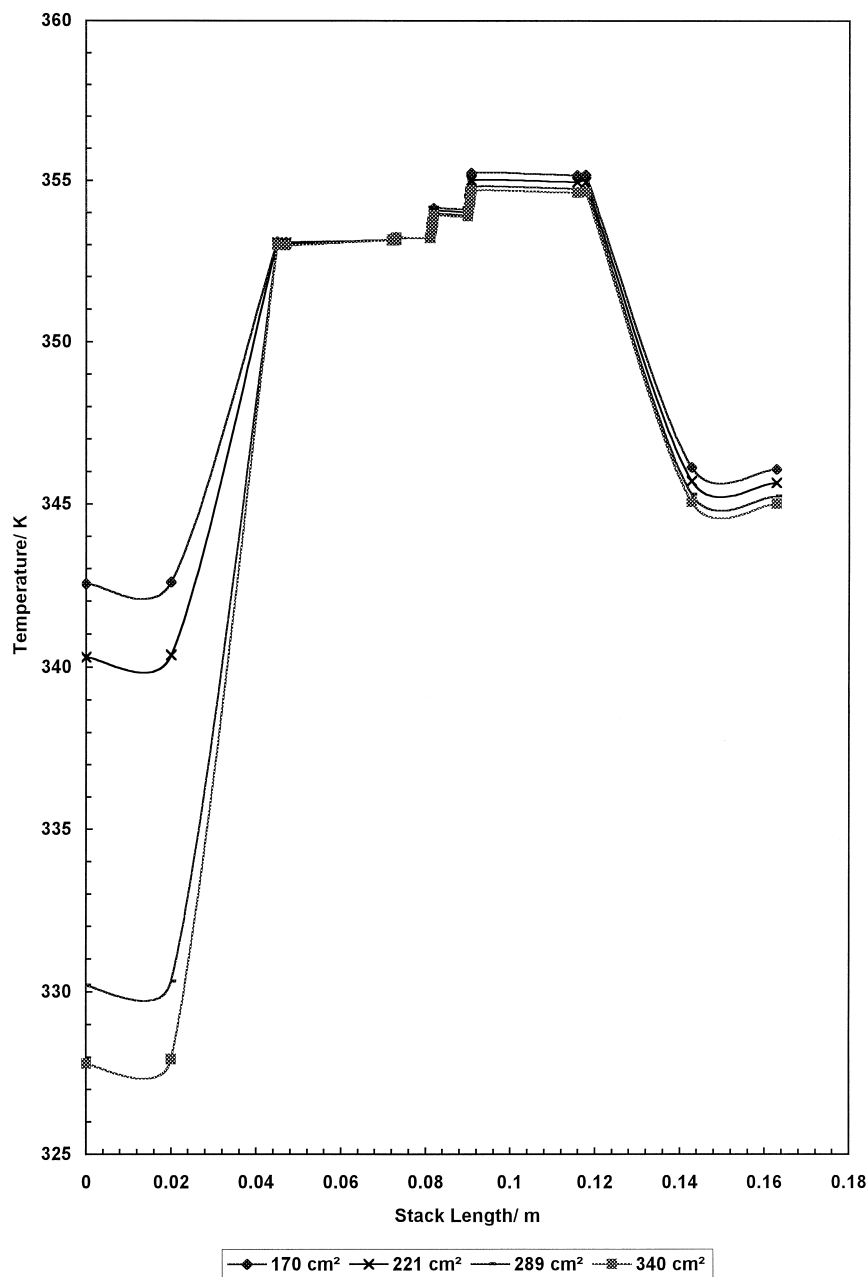


Fig. 4. Three-cell stack longitudinal temperature profiles for increasing electrocatalytically active area ( $170\text{--}340\text{ cm}^2$ ) for the same block cross-section area at  $80^{\circ}\text{C}$  anode side inlet temperature,  $20^{\circ}$  cathode side inlet temperature, current density  $100\text{ mA cm}^{-2}$ , anode inlet flow rate  $1.0\text{ dm}^3\text{ min}^{-1}$  per cell, cathode inlet flow rate  $2.0\text{ dm}^3\text{ min}^{-1}$  per cell, 2 bar cathode pressure.

in the fluid flow to each individual cell, which will thus effect the local transfer of heat in each cell and thus the operating temperatures of the cell components.

Probably the most important factor in fuel cell operation is the current density. Increasing current density results in an increase in the rate of consumption of reactants, in the formation of products, in water and methanol crossover, and in joule heat. In other words in the amount of heat produced and on how the heat is transferred in the stack structure particularly as electroosmotic drag is a major heat transfer mechanism. Figs. 2 and 3 show the influence of operating current density on the stack temperature profile. Fig. 2 is based on a 1:1 ratio of feed and oxidant inlet flow rates ( $1.0 \text{ dm}^3 \text{ min}^{-1}$ ), while in Fig. 3 the oxidant flow rate is increased to  $2.0 \text{ dm}^3 \text{ min}^{-1}$ . A reason for increasing the flow rate, in the case of Fig. 3, was that the lower flow rate of  $1.0 \text{ dm}^3 \text{ min}^{-1}$  was not sufficient to maintain operation for current densities above  $400 \text{ mA/cm}^2$ . Such an air supply is very close to that stoichiometrically needed to maintain operation around  $300 \text{ mA/cm}^2$ . Thus, by increasing the operating current density the cell consumes all the available air quantity, which is not sufficient to maintain operation. The small difference between the two sets of data can be explained from the small effect that the air inlet flow rate has on the stack predicted temperature profile.

As expected increasing the current density quite dramatically affects the average stack temperature ( $20^\circ\text{C}$  for an increase from  $100$  to  $700 \text{ mA/cm}^2$ ). Thus operating in high current densities will result in increased thermal management problems, due to the high amount of heat produced. These problems for liquid fed cells include vaporisation of the methanol feed, if operating under near atmospheric pressure conditions. The aspect of fuel vaporisation has not been included specifically in the model at this stage.

A third important design parameter in the fuel cell is the active cross-section area within the fuel cell. It is assumed that the active area and the flow bed cross-section area are the same (which is normally true). By increasing the active area there is an increase in the heat transfer area between the fluids and the stack materials and also an increase in the amount of heat generated in the cell and the amount of heat transferred by electro-osmotic flow. The method of increasing the active area is by keeping the flow bed width constant and increasing its length, whilst we maintain a constant stack cross-section ( $0.25 \text{ m} \times 0.25 \text{ m}$  in our case). Thus, in this way, the losses from the stack-exposed area to the environment are constant and dependent only upon the exposed area and the stack temperature. Fig. 4 shows that there is a small decrease in the average temperature for an increase in the active area. This trend can be explained from the fact that important system parameters, such as water and methanol crossover, stack current, and heat produced, are also active area dependent and that in all cases the inlet flow rates are kept constant. The air

inlet-stream is the main external mechanism for heat removal from the stack main body, since the anode inlet stream is preheated to a temperature close to the stack average temperature and thus has limited heat removal ability. In every cell, the area for convective heat transfer is the same one with the active area. Hence, the smaller this area becomes, the smaller the heat removal rate from the cathode side. This results in an increase in the overall temperature profile. Nevertheless, the amount of heat carried away from the cathode stream is relative small, and accordingly the difference in the stack temperature is very small (less than  $0.5^\circ\text{C}$ ) even for a 100% increase in the active area. It should be noted that although there is only a small effect, of the active area ratio to the stack cross-section, on the stack heat management it is important for the system designer to maximise this ratio. This will result in a system with a high degree of compactness, and high ratio of electrical energy produced to stack mass, which is important for vehicular traction applications [4–12].

#### 4. Anode side related parameters

The anode is the most critical side of the fuel cell since it determines the overall temperature profile. This is because the anode stream is the main mechanism of heat supply for the anodic endothermic reaction. Accordingly, the cell's electrochemical performance depends on the rate of that reaction. Furthermore, this stream is liquid and thus has a high thermal capacity combined with high heat transfer ability, in comparison to the cathode side. The effect of two anode side inlet stream related parameters: methanol solution flow rate and inlet temperature, are considered below.

Fig. 5 shows the temperature profiles for increasing anode inlet flow rate. Increasing the anode side flow rate increases the stack temperature to a limited extent because the main heat transfer mechanism (electroosmotic flow) and the main heat production mechanism (cathodic reaction) are independent of the liquid flow rate. The small increase in the temperature is a result of the increase in the convective heat transfer coefficient, which, for the case of a plate heated to its full length, and in laminar flow without phase change is: If  $\text{Gr} > 10^9$

$$\text{Nu} = 0.138\text{Gr}^{0.36}(\text{Pr}^{0.175} - 0.55) \quad (1)$$

and if  $\text{Gr} < 10^9$

$$\text{Nu} = 0.683\text{Gr}^{0.25} \left( \frac{\text{Pr}}{0.861 + \text{Pr}^{0.25}} \right) \quad (2)$$

This equation is valid for Prandtl numbers of 1.0 or greater, since the derivation assumes a thermal boundary layer no thicker than the hydrodynamic layer. However, they can be used for gases with  $\text{Pr} = 0.7$  with little error [13,14]. Hence, due to the flow rate increase (higher Reynolds number), the amount of heat transferred through

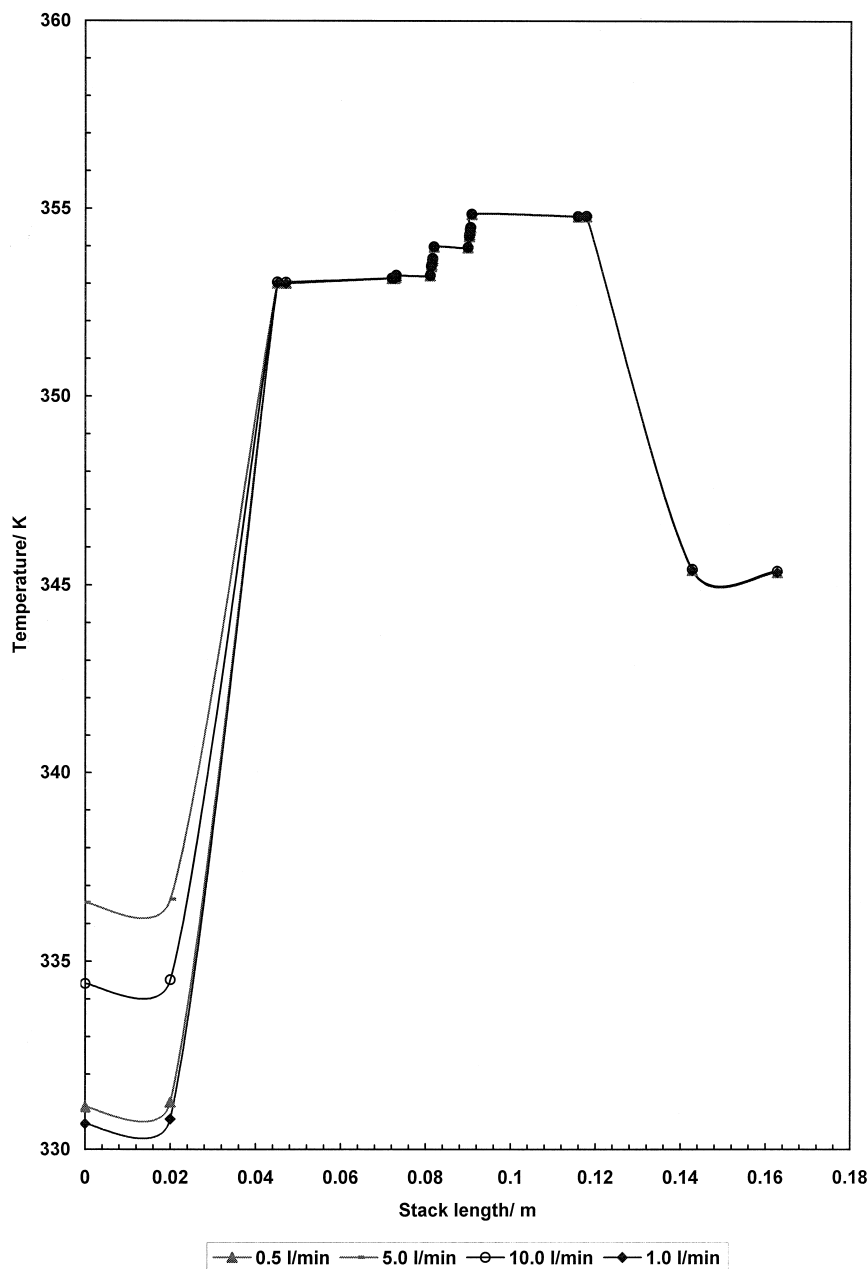


Fig. 5. Three-cell stack longitudinal temperature profiles for increasing anode side inlet flow rate ( $0.5\text{--}10\text{ dm}^3\text{ min}^{-1}$ ) at  $80^\circ\text{C}$  anode side inlet temperature,  $20^\circ$  cathode side inlet temperature, current density  $100\text{ mA cm}^{-2}$ , cathode inlet flow rate  $2.0\text{ dm}^3\text{ min}^{-1}$  per cell, 2 bar cathode pressure.

that mechanism towards the membrane electrode assembly is increased. Unfortunately, the low heat transfer coefficient, combined with the small heat transfer area, mean the heat added from this mechanism is small.

An important additional practical point in DMFC fuel cell stack operation is that higher liquid flow rates result in more efficient carbon dioxide removal. This has been observed in flow visualisation studies to be reported in detail elsewhere [15,16], where there is evidence that carbon dioxide is more rapidly removed from the flow channels at higher flow rates. Hence, in practical operation, this will lead to an increase in the cell stack electrical performance [15,16].

In the case when the stack body is at a higher temperature than the anode inlet stream, the anode inlet stream will act as a cooling liquid, and will no longer supply heat to the stack but will remove it. Then obviously increasing the liquid flow rate will result in a small drop in the stack's temperature profile. The optimal flow rate will eventually be a compromise between the pumping requirements, the energy for heating the methanol feed, the stack cooling requirements and the required stack power performance.

A key parameter, which determines the stack operating temperature, is the inlet temperature of the methanol solution, (based on an adequate solution flow rate). Figs. 6 and 7 depict the effect of methanol solution feed temperature

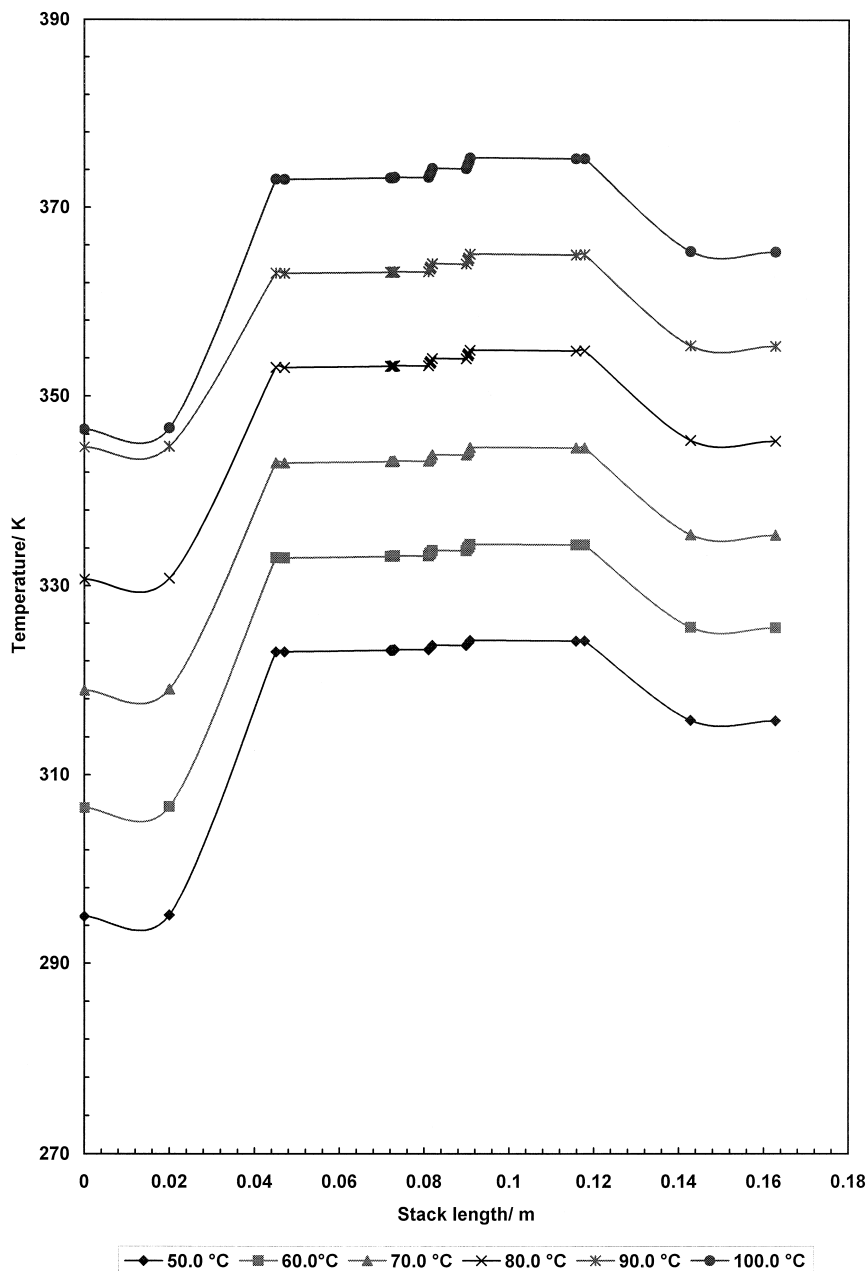


Fig. 6. Three-cell stack longitudinal temperature profiles for anode side inlet temperature (50–100°C) at 20°C cathode side inlet temperature, current density  $100 \text{ mA cm}^{-2}$ , anode inlet flow rate  $1.0 \text{ dm}^3 \text{ min}^{-1}$  per cell, cathode inlet flow rate  $2.0 \text{ dm}^3 \text{ min}^{-1}$  per cell, 2 bar cathode pressure.

on the stack temperature profile. Fig. 6 is for a three cell-stack and Fig. 7 for a 10-cell stack. It is clear that the steady state temperature of the stack, with a small number of cells, will be around the inlet methanol feed temperature. Of course for a stack containing a larger number of cells then this conclusion is not longer valid (Fig. 7); the temperature variation can be between 10 and 20°C, depending upon the anode side inlet temperature. However in general the lower temperature of the stack is determined again by the methanol feed inlet temperature.

Based on the aforementioned results a maximum allowable stack temperature controlling strategy can be adopted.

Since that maximum, to a large extent, depends on the liquid phase inlet temperature a PLC controller can be used which will control the anode side liquid temperature as a function of the maximum stack temperature. The controller can be programmed with the aid of a more sophisticated combined hydraulic-thermal model for a stack with a predetermined design. Reducing the anode side inlet temperature (i.e., by reducing the heater outlet temperature) will lower quickly the average stack temperature. Despite the fact that according to the present model the anode side inlet flow rate doesn't seem to affect the predicted temperature profile a recent model developed by



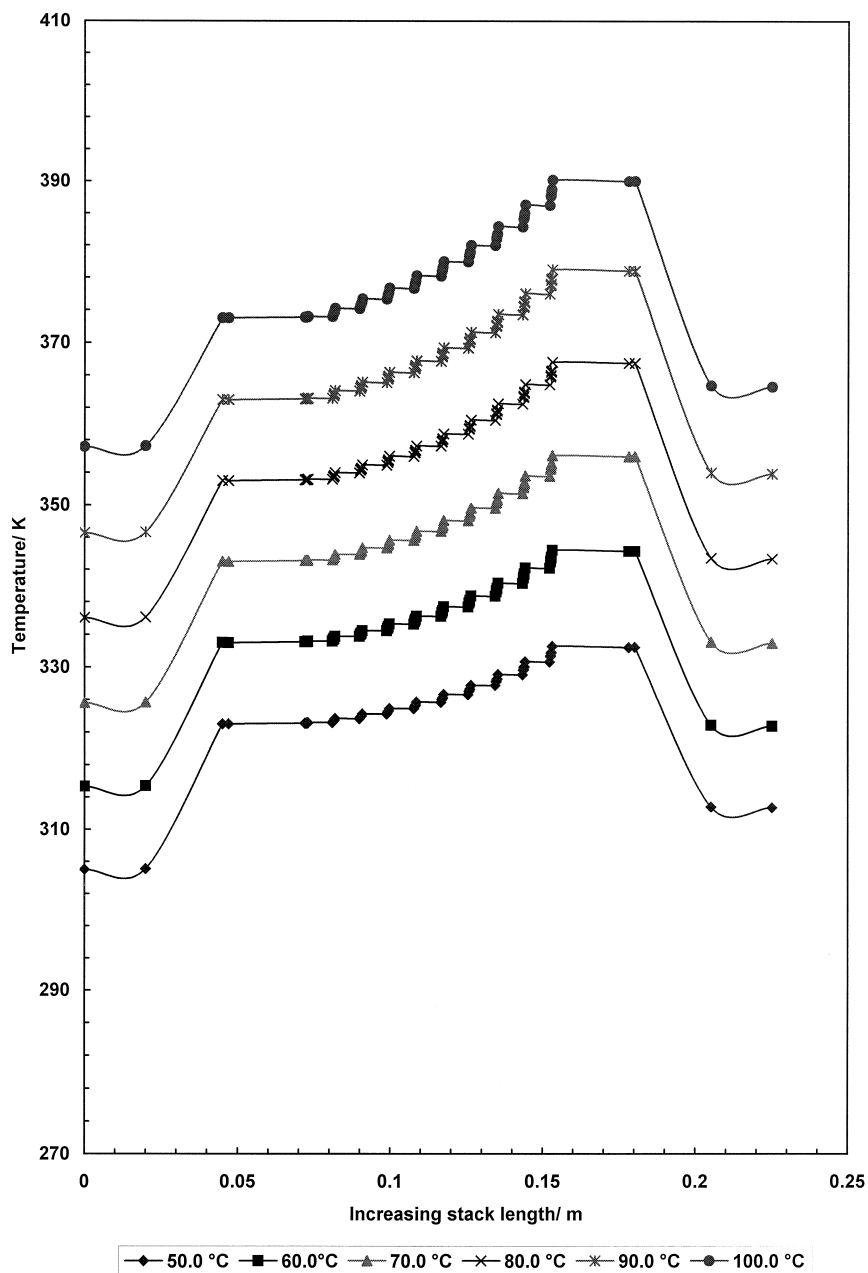


Fig. 7. Ten-cell stack longitudinal temperature profiles for anode side inlet temperature (50–100°C), at 20°C cathode side inlet temperature, current density  $100 \text{ mA cm}^{-2}$ , anode inlet flow rate  $1.0 \text{ dm}^3 \text{ min}^{-1}$  per cell, cathode inlet flow rate  $2.0 \text{ dm}^3 \text{ min}^{-1}$  per cell, 2 bar cathodic pressure.

our group revealed that the flow distribution inside a DMFC stack can vary to a very large extent [17]. The poor prediction of the present model is due to the fact that it is based on the assumption that all the cells are equally fed. Hence, a combination of anode side inlet flow rate and feed inlet temperature can help in controlling and removing effectively the excess heat. Currently, we are developing a model that takes under consideration the thermal, hydraulic and chemical behaviour of our prototype stack, which is hoped will be quite accurate in predicting the stack behaviour.

A final comment should be made on the heat losses in the end block. These losses are strongly dependent on the

adjacent cell average temperature and the flow rate of the fluid flowing in the end block flow bed. Though generally not very critical, they could become an important issue in the case of insufficient thermal insulation or a thermal insulation failure.

## 5. Cathode side related parameters

The cathode side air stream generally acts as a means of convective heat transfer from the cell stack but is of limited importance (at practical flow rates) due to the

relatively low heat capacity of air. As can be seen in Figs. 8 and 9 the air inlet temperature and the air volumetric flow rate have only a small influence on the temperature profile of the stack. Increasing the cathode side inlet temperature (Fig. 8) tends to flatten the temperature profile as the stack approaches a fully isothermal system. The model has an embedded mechanism that accounts for the variation of the physical properties with temperature for both anode and cathode fluids. Since gas properties are greatly affected by temperature (especially density and hence Reynolds number) in the case of low inlet temperatures the benefit from an increase in the overall side

gradient is lost from the change in the physical properties and the decrease in all the related parameters. In other words, the higher mean gas temperature not only decreases the temperature gradient between the gas and the graphite block, but also decreases the cathode side heat transfer coefficient and thus convective heat removal. This results in decreased heat removal efficiency.

As expected an increase in the air volumetric flow rate results in a small decrease in the stack's temperature profile. This effect may be unwanted in the case of very high flow rates since it leads to a localise cooling of the active area (which is made from highly conductive materi-

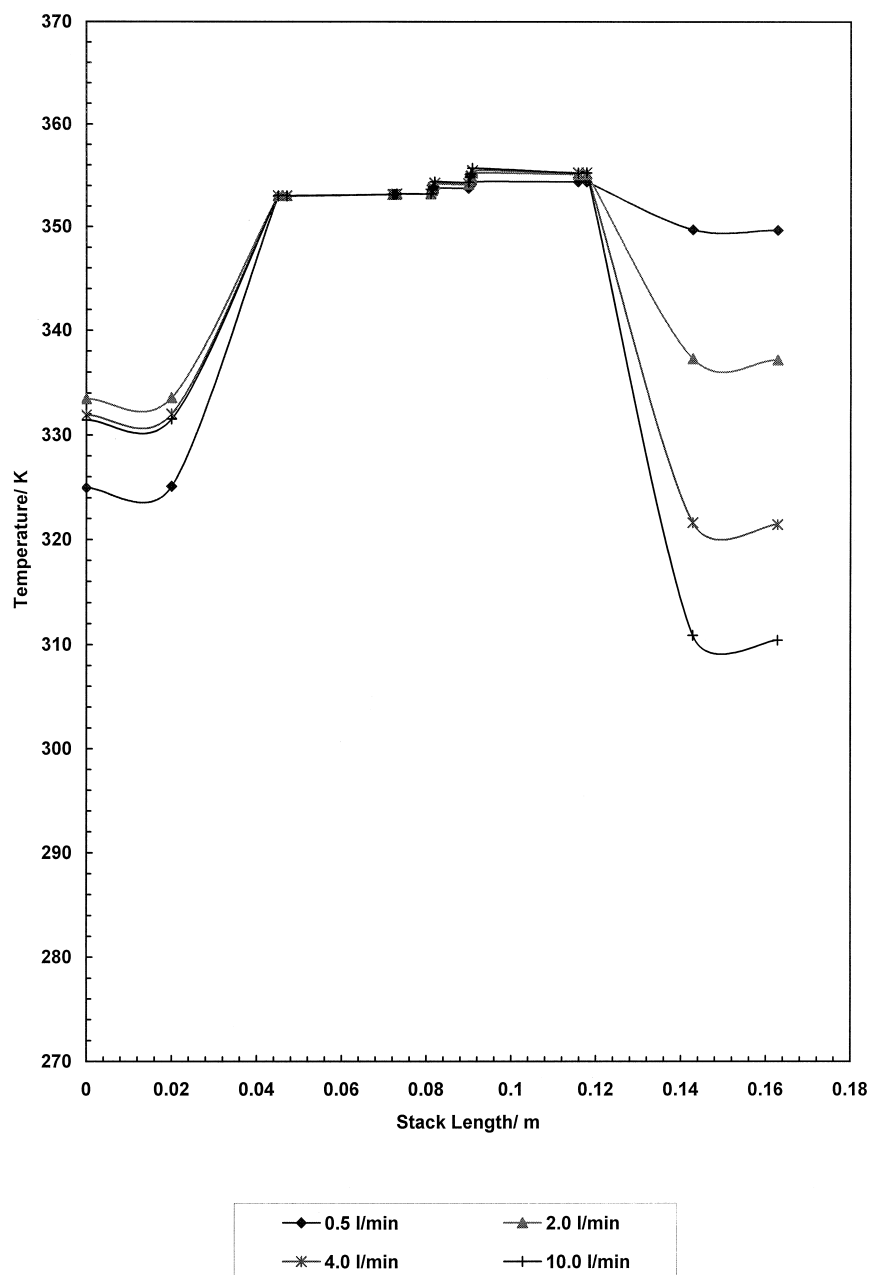


Fig. 8. Three-cell stack longitudinal temperature profiles for increasing cathode side inlet flow rate ( $0.5\text{--}10\text{ dm}^3\text{ min}^{-1}$ ) at  $80^\circ\text{C}$  anode side inlet temperature,  $20^\circ$  cathode side inlet temperature, current density  $100\text{ mA cm}^{-2}$ , anode inlet flow rate  $1.0\text{ dm}^3\text{ min}^{-1}$  per cell, 2 bar cathode pressure.

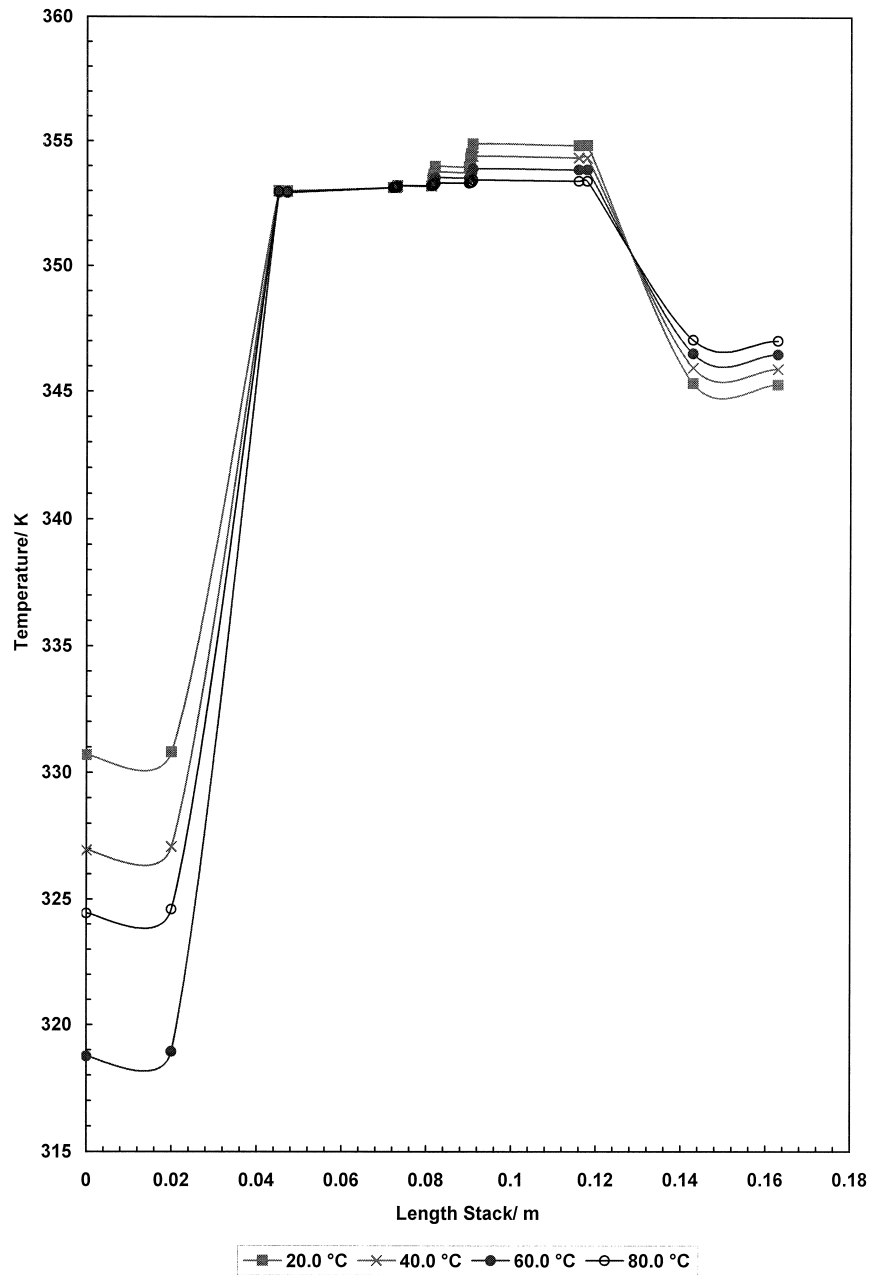


Fig. 9. Three-cell stack longitudinal temperature profiles for cathode side inlet temperature (20–80°C) at 80°C anode side inlet temperature, current density  $100 \text{ mA cm}^{-2}$ , anode inlet flow rate  $1.0 \text{ dm}^3 \text{ min}^{-1}$  per cell, cathode inlet flow rate  $2.0 \text{ dm}^3 \text{ min}^{-1}$  per cell, 2 bar cathode pressure.

als). High air flow rates are beneficial in solving the cathode water-flooding problem, which occurs typically at high current densities. This problem is reported from various groups [3] and is created by the difficulty in removing water from the porous cathode. This results in deterioration in performance, since the oxidant is not able to fully penetrate (diffuse to) the reaction sites. Although cathode flooding can be remedied by increasing the oxidant flow rate, (with all the unwanted side effects) we have found it beneficial to make use of the gravitational force to help alleviate this problem. This is achieved by adopting a downwards cathodic flow configuration [18,19].

Overall, the analysis again points to the logical conclusion that the decision on cathode operating conditions will be based on a compromise on energy requirement for compressing air, air heating requirements (if needed), cathode side water management, and stack thermal management requirements. The current stack thermal model can be used as a tool in this decision making and optimisation.

## 6. Anode and cathode outlet temperatures

In the operation of the fuel cell stack, the outlet temperatures of the fuel and oxidant streams determine require-

ments for fuel recycling, and recovery, and heat recovery. A high fuel exit temperature will reduce the solubility of carbon dioxide in the methanol solution and create more methanol and water vapour in the gas stream. The recovery and re-use of this methanol is important in terms of fuel utilisation efficiency and becomes more critical, and difficult, with a higher temperature of the fuel exit stream as more methanol vapour is present. In addition because of methanol crossover from the anode to cathode there will be methanol present in the exhaust oxidant stream. The quantity of methanol in this stream is significantly less than that in the carbon dioxide off gas from the anode side

of the cell and it becomes questionable whether or not it is economic to separate the methanol for re-use in the fuel cell. In both cases, the removal of the majority of the methanol from the gas stream is unlikely to be achievable with, for example air cooled, condensers, because of the presence of the non-condensable gases; either carbon dioxide or nitrogen and oxygen. In a separate modelling study of the fuel cell operation estimations of required condensation temperatures for near complete removal of the methanol from the carbon dioxide off-gas are around  $-40$  to  $-60^{\circ}\text{C}$  which are clearly not economic. Thus, an alternative strategy is required where an alternative process

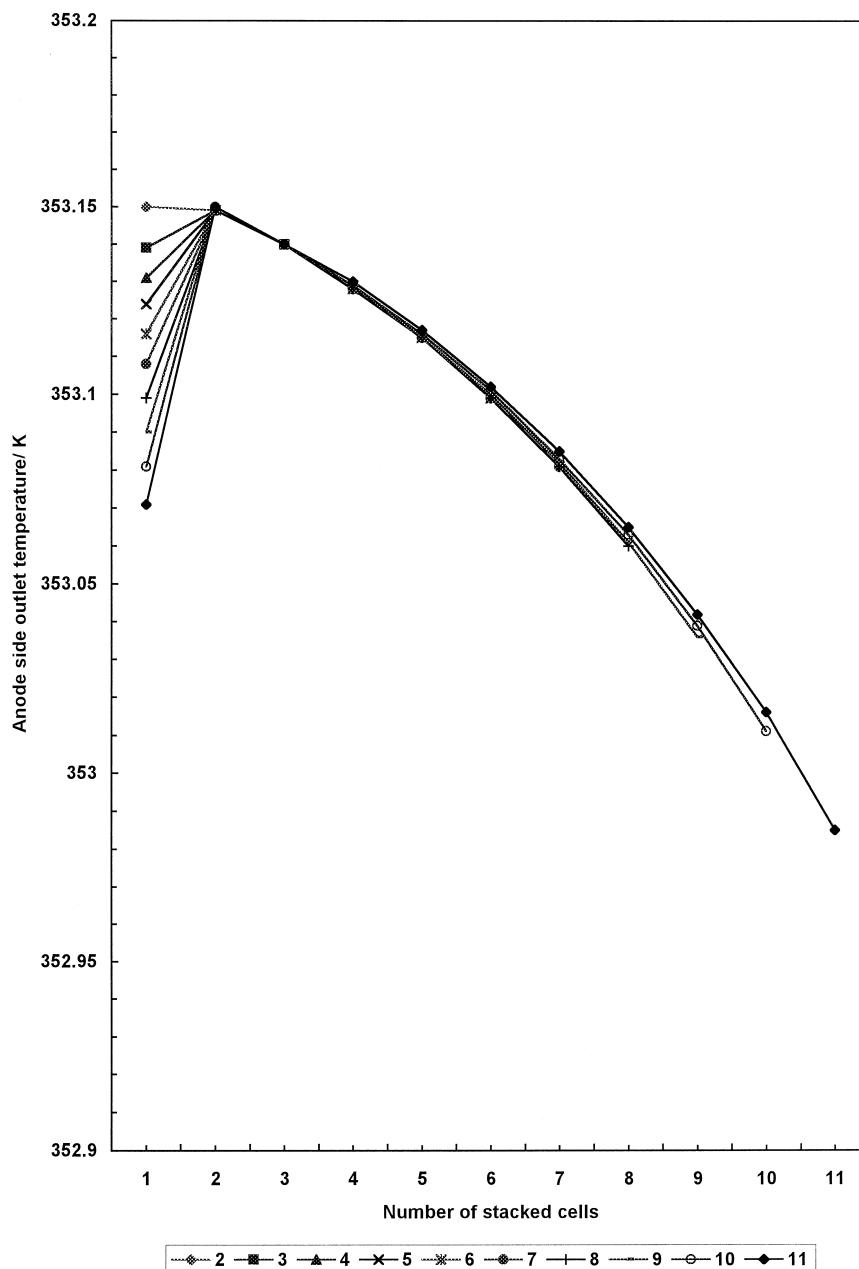


Fig. 10. Anode side outlet temperature as a function of increasing number of stacked cells (1–11) at  $80^{\circ}\text{C}$  anode side inlet temperature,  $20^{\circ}$  cathode side inlet temperature, current density  $100\text{ mA cm}^{-2}$ , anode and cathode inlet flow rate  $1.0\text{ dm}^3\text{ min}^{-1}$  per cell, 2 bar cathode pressure.

or where residual methanol is combusted achieves separation. These issues are beyond investigation in the current study but do highlight the need for suitable modelling of the fuel cell stack thermal characteristics [2,20].

Fig. 10 shows the variation in the anode solution exit temperature with the number of cells in the stack (2 to 11 cells). The anode methanol flow rate is  $1.0 \text{ dm}^3/\text{min}$ , the inlet temperature is  $80^\circ\text{C}$  and the operating current density is  $100 \text{ mA}/\text{cm}^2$ . The fluid temperature from the second cell is always the largest for all the cells. This is due to the effect of heat transfer from the anode side end block. The

anode side outlet temperature, after the second cell, slightly decreases with an increasing number of cells present in the stack. This is due to a number of reasons: increased heat losses to the surroundings (the exposed area is bigger and the stack average temperature is higher), increase in the cathode side outlet temperature (see Fig. 11). The losses should be replenished from the liquid heat content, since the heat produced from the cathodic exothermic reaction is mainly consumed in vaporising the liquid water and methanol present at the cathode catalyst layer. Overall, due to the small convective heat transfer coefficient, the negli-

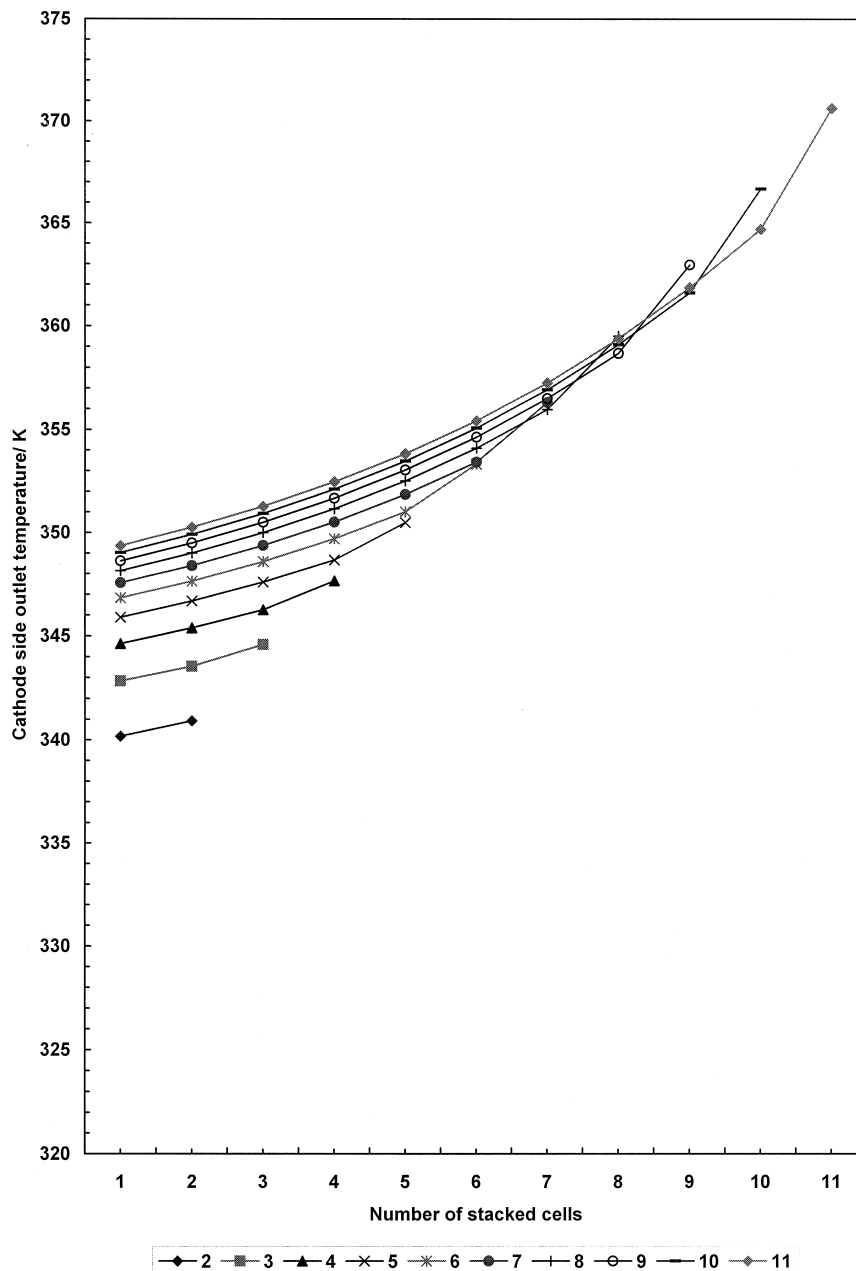


Fig. 11. Cathode side outlet temperature as a function of increasing number of stacked cells (1–11) at  $80^\circ\text{C}$  anode side inlet temperature,  $20^\circ$  cathode side inlet temperature, current density  $100 \text{ mA cm}^{-2}$ , anode and cathode inlet flow rate  $1.0 \text{ dm}^3 \text{ min}^{-1}$  per cell, 2 bar cathode air pressure.

Table 1  
Summary of model results

Parameter	Effect on stack temperature profile	Comments
Increasing the number of stacked cells	Increase	Critical parameter
Increasing the ratio of active to total cross sectional area	Small	–
Increasing the current density	Increase	Critical parameter
Increasing the anode side inlet temperature	Increase	Critical parameter
Increasing the anode side inlet flow rate	Small increase	Convective heat transfer not critical
Increasing the cathode side inlet temperature	Increase	Weak effect
Increasing the cathode side inlet flow rate	Small decrease	Due to model assumptions (see above)

gible temperature difference and the large volumetric flow rate, even when the cell temperature is higher than the anode side average temperature there is no significant heat removal from the anode side and hence there is not a significant variation in anode solution exit temperature ( $< 1^{\circ}\text{C}$ ).

Fig. 11 shows the variation in the cathode exhaust temperature with the number of cells in the stack (2 to 11 cells). The cathode air temperature increases drastically with an increasing number of cells in the stack. This is expected since increasing the number of cells has as the effect of increasing the stack temperature profile. In addition, heat is transferred from the anode to the cathode side of the cell and whatever heat not removed in the cathode air stream is carried over to the next cell.

Overall, the amount of heat transferred from the liquid to the membrane electrode assembly is critical for the cell's operation. Although small this amount of heat is important because of the relatively small heat capacity of the whole electrode assembly. The model data highlight the heat removal problems associated with stack operation with a large number of cells present in the stack.

## 7. Conclusions

A mathematical model is used to estimate temperature profiles and heat flows in a liquid feed DMFC stack and to enable decisions to be made on thermal management strategy. Heat production and heat losses to the surroundings are calculated with the aid of a one-dimensional steady state thermal model based on the energy conservation equation. In the stack system design, the number of the cells present in the stack and the operating current density are two of the most critical parameters for thermal management. Increasing either of these two factors results in a significant increase in the overall stack temperature gradient.

The anode side inlet temperature is of importance in determining the stack temperature profile. Other factors, such as the fuel and oxidant flow rates and the cathode side inlet temperature are of less importance, at least in the range of operating conditions that are economically viable

and technically feasible, as studied in this paper. The model results are summarised in Table 1.

## Acknowledgements

The authors would like to acknowledge the following: (1) The European Commission for supporting Mr. P. Argyropoulos under a TMR Marie Curie research training grant; (2) EPSRC for supporting Dr. W.M. Taama.

## References

- [1] K. Scott, W.M. Taama, P. Argyropoulos, Material aspects of the liquid feed direct methanol fuel cell, *J. Appl. Electrochem.* 28 (1998) 1384.
- [2] K. Scott, W.M. Taama, P. Argyropoulos, Engineering aspects of the direct methanol fuel cell system, Accepted for publication in *J. Power Sources*, 1998.
- [3] T.I. Valdez, S.R. Narayanan, H. Frank, W. Chun, Direct methanol fuel cell for portable applications, in: *Annual Battery Conference on Applications and Advances*, Long Beach, USA, 1997.
- [4] C.E. Borroni-Bird, Fuel cell commercialization issues for light duty vehicle applications, *J. Power Sources* 61 (1996) 33–48.
- [5] S.G. Chalk, J. Milliken, J.F. Miller, S.R. Venkateswaran, The US Department of Energy—investing in clean transport, *J. Power Sources* 71 (1998) 26–35.
- [6] S.G. Chalk, P.G. Patil, S.R. Venkateswaran, The new generation of vehicles: market opportunities for fuel cells, *J. Power Sources* 61 (1996) 7–13.
- [7] F. Du Melle, The global and urban environment: the need for clean power systems, *J. Power Sources* 71 (1998) 7–11.
- [8] C.E. Gibbs, M.C.F. Steel, European opportunities for fuel cell commercialization, *J. Power Sources* 37 (1992) 35–43.
- [9] D.R. Glenn, Direct fuel cell power plants: the final steps to commercialisation, *J. Power Sources* 61 (1996) 79–85.
- [10] M.P. Hogarth, G.A. Hards, Direct methanol fuel cells. Technological advances and further requirements, *Platinum Met. Rev.* 40 (4) (1996) 150–159.
- [11] H. Ledjeff, A.K. Heinzl, Critical issues and future prospects for solid polymer fuel cells, *J. Power Sources* 61 (1996) 125–127.
- [12] X. Ren, S.C. Thomas, P. Zelenay, S. Gottesfeld, Direct methanol fuel cells: developments for portable power and for potential transportation applications, in: *1998 Fuel Cell Seminar*, Palm Springs, CA, USA, 1998.
- [13] W.L. McCabe, J.C. Smith, P. Harriott, *Unit Operations of Chemical*

- Engineering, 5th International edn., McGraw-Hill Chemical Engineering Series, McGraw-Hill, Singapore, 1995.
- [14] R.H. Perry, D.W. Green, D.J.O. Maloney, Perry's Chemical Engineers' Handbook, 6th International edn., McGraw-Hill, Singapore, 1984.
- [15] P. Argyropoulos, K. Scott, W.M. Taama, Carbon dioxide evolution patterns in operating DMFC cells, *Electrochim. Acta*, 1998, in press.
- [16] P. Argyropoulos, K. Scott, W.M. Taama, Gas evolution and power performance in direct methanol fuel cells, *J. Appl. Electrochem.*, 1999, in press.
- [17] P. Argyropoulos, K. Scott, W.M. Taama, Pressure drop modelling for liquid feed direct methanol fuel cells (DMFCs): Part II. Model based parametric analysis, *Chem. Eng. J.*, 1999, in press.
- [18] P. Argyropoulos, K. Scott, W.M. Taama, Modelling reactants and products flow distribution for internally manifolded DMFC stacks, Submitted to the *J. Fluids Eng.*, 1998.
- [19] P. Argyropoulos, K. Scott, W.M. Taama, Pressure drop modelling for liquid feed direct methanol fuel cells (DMFCs): Part I. Model development, *Chem. Eng. J.*, 1999, in press.
- [20] K. Sundmacher, K. Scott, Direct methanol polymer electrolyte fuel cell: analysis of charge and mass transfer in the vapour–liquid–solid system, *Chem. Eng. Sci.*, 1999, in press.